EVOLUTION OF NUCLEAR STRUCTURE WITH INCREASING SPIN AND INTERNAL EXCITATION ENERGY IN ^{152}Dy ☆

R. HOLZMANN, I. AHMAD, B.K. DICHTER, H. EMLING [1], R.V.F. JANSSENS, T.L. KHOO, W.C. MA
Argonne National Laboratory, Argonne, IL 60439, USA

M.W. DRIGERT, U. GARG
University of Notre Dame, Notre Dame, IN 46556, USA

D.C. RADFORD
Chalk River Nuclear Laboratories, Chalk River, Ontario, Canada K0J 1J0

P.J. DALY, Z. GRABOWSKI, H. HELPPI [2], M. QUADER and W. TRZASKA
Purdue University, West Lafayette, IN 47907, USA

Received 23 June 1987

The total γ ray spectrum emitted by ^{152}Dy has been measured in two different reactions and decomposed into its constituent parts. From the measured decay times, multiplicities, multipolarities and spectral shapes, the average decay path has been reconstructed. The yrast single-particle structures have been shown to give way to highly collective bands at internal excitation energies > 1.5 MeV. A model, which takes into account the competition between statistical and collective decay at high spin and temperature, has been used to fit all features of the data, yielding $Q_t = 7.0^{+2.5}_{-1.5}$ *e* b for the collective bands.

The evolution of nuclear properties with changing angular momentum (I) and internal excitation energy (U), i.e. energy above the yrast line, is a major theme in nuclear research. Structural changes due to alterations in the shell effects, brought about by the varying occupation of the single-particle orbits, can be probed by tracing the γ cascades in the spin versus excitation-energy plane and by measuring the lifetimes of the transitions involved.

The nucleus ^{152}Dy is ideal for such investigations. Its yrast and near-yrast states are mainly of single-particle nature up to very high spins [1,2], whereas above the yrast line there are discrete-line rotational bands with $\beta = 0.15$ and $\beta = 0.6$ [3,4]. Furthermore, studies of the γ-ray quasicontinuum [5–7] suggest the existence of collective states at higher excitation energy which give rise to the so-called E2 bump. These features imply a major change of nuclear structure with U. The discrete-line bands account for only a small fraction (< 6%) of the total γ-ray intensity and the bulk of the collective transitions are in the strong E2 bump. Clearly, it is important to ascertain if these collective transitions are connected with the recently observed superdeformed $\beta = 0.6$ band [4]. The nature of these transitions, their location and extent in spin and excitation energy, and the nature of the evolution from the collective to the single-particle states remain to be determined.

This letter reports on a comprehensive study of the quasicontinuum γ radiation. We have measured the total γ-ray spectrum from ^{152}Dy and decomposed it

☆ This work was supported by the Department of Energy under Contracts Nos. W-31-109-Eng-38 and DE-AC02-76ER01672, and by the National Science Foundation under Grant No. PHY84-16025.

[1] Present address: GSI, D-6100 Darmstadt, Fed. Rep. Germany.

[2] Present address: Lappeenranta University, SF-53851 Lappeenranta, Finland.

0370-2693/87/$ 03.50

into its constituent parts [8]. For the first time lifetime information on *all* parts has been obtained and their time sequence ascertained. Another new aspect of this work is that all observed features – lifetimes, spectral shapes, multipolarities and multiplicities – of different components of the quasicontinuum are treated simultaneously and can be *quantitatively* described in a simple γ-cascade calculation. (A discussion of $E_\gamma - E_\gamma$ correlations is deferred to a later publication.) Whereas only some isolated aspects of the quasicontinuum spectrum have been described in the literature – often in qualitative terms – we now quantitatively describe the full deexcitation cascade. Thus, we can infer how the nuclear structure changes as a function of both I and U.

To obtain such quantitative data on the quasicontinuum transitions it is imperative to disentangle their properties from those of the strong yrast transitions. This is not possible using only NaI detectors – and hence was done only in a few cases in earlier work – but can be reliably done with the use of Compton-suppressed Ge (CSG) detectors, as has been argued in ref. [8].

We produced ^{152}Dy using the ^{76}Ge(^{80}Se, 4n) and ^{120}Sn(^{36}S, 4n) reactions with beams provided by the Argonne superconducting linac, ATLAS. The effective beam energies were 311 MeV for ^{80}Se and 157 MeV for ^{36}S, resulting in recoil velocities $v/c = 0.047$ and 0.020, respectively, for the residual nuclei. In a first experiment prompt γ rays were measured in four BGO CSG's of the Argonne–Notre Dame γ-ray facility, positioned at 0°, 45°, 90° and 147° with respect to the beam axis. An array of 14 NaI crystals provided both enhancement of high-multiplicity events and clean selection of a single reaction channel, through tagging on the ^{152}Dy 60 ns isomer [1]. In a second experiment, eight CSG's placed at 34°, 90° and 146° were used together with an array of 14 hexagonal BGO crystals. In order to extract lifetime information, data were accumulated for two different sets of thin (~ 0.5 mg/cm^2) targets: (i) self-supporting foils where the residual nuclei recoiled into vacuum, yielding spectra which were fully Doppler-shifted and which could thus be decomposed into their constituent parts without complications from lifetime effects; (ii) foils evaporated on a 50 mg/cm^2 thick backing material (Au in the first experiment and Pb in the second) which stopped the recoiling nuclei within ~ 1.6 ps, producing energy shifts dependent on the characteristic emission times of the different spectral components.

Both data sets were analyzed identically. Contaminant γ rays from ^{151}Dy, present because of its 13 ns isomer, and random delayed coincidences were removed by subtracting spectra with appropriate time gates. A correction for coincidence-summing was applied and a measured neutron-induced background was subtracted [9]. The resulting spectra were unfolded and corrected for the photopeak efficiency [10], yielding the prompt γ-ray spectrum emitted by ^{152}Dy with no contributions from any other nuclei.

Fig. 1a shows the spectrum for the ^{80}Se + ^{76}Ge reaction measured at 0° with the backed target. Following the classification scheme proposed in ref. [8], the total spectrum has been decomposed into: (i) discrete lines corresponding to transitions assigned in the level scheme of ^{152}Dy [1,3,4] (called "trees"); (ii) weak ($I_\gamma < 2\%$) unassigned peaks ("grass"); (iii) the underlying continuum ("soil"); and (iv) the statistical γ rays, fitted between 2.5 and 4.5 MeV with the usual expression $E_\gamma^3 \exp(-E_\gamma/T)$, with $T = 0.5$ MeV. The grass and soil components were further decomposed into dipole and quadrupole parts (see fig. 1b) using the average A_2 and A_4 coefficients deduced from the measured angular distributions, under the assumption of stretched transitions. The A_2 value for the dipole soil actually implies $\sim 10\%$ quadrupole admixture, suggesting a dominant M1 multipole.

The average multiplicity $\bar{M}_\gamma$ of each component was determined by integrating an appropriately normalized spectrum. The average removed spin, $\overline{\Delta I} = \bar{M}_\gamma \cdot \lambda$, and energy, $\overline{\Delta E} = \bar{M}_\gamma \cdot \bar{E}_\gamma$, could then be computed. The results for the two reactions measured are summarized in table 1 together with the deduced average entry spins and entry excitation energies. It is apparent that an increase in average entry spin from 47 $\hbar$ to 55 $\hbar$ results mainly in an increase of the E2 soil multiplicity, whereas the multiplicity and spectral shape of the dipole soil are virtually unaffected (see also fig. 1b).

Emission times of the different spectral components were derived by comparing the Doppler shifts and yields (which reflect the aberration effect) measured with the backed and unbacked targets. A few results from this work is that the dipole soil com-

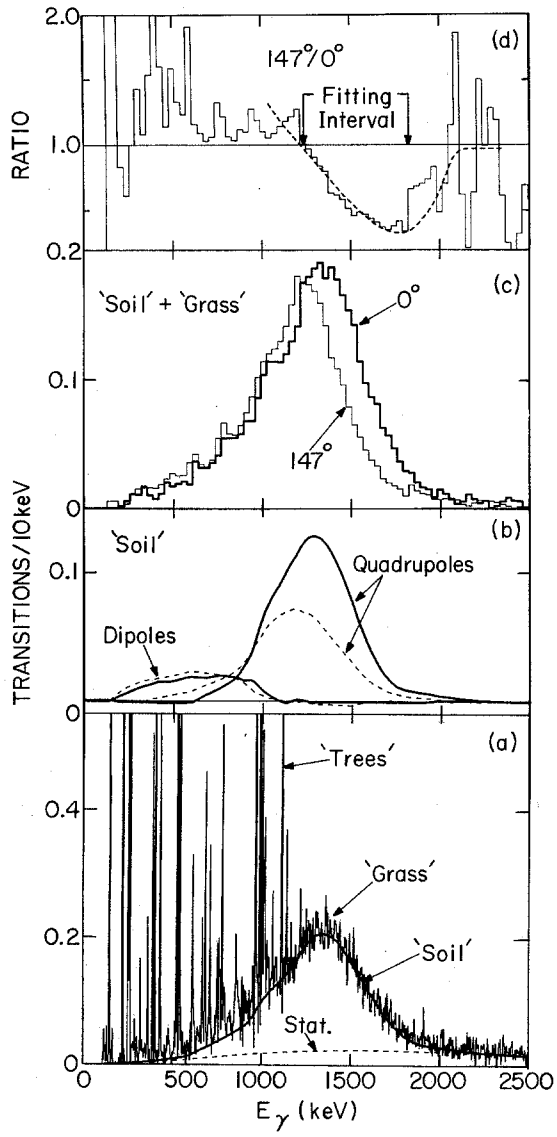

Fig. 1. Unfolded γ spectra from the reaction ^{67}Ge(^{80}Se, 4n)^{152}Dy at 311 MeV measured with a backed target. (a) Total spectrum measured at 0°. The dashed line shows the statistical component, obtained by fitting the spectrum between between 2.5 and 4.5 MeV with the expression $E_\gamma^3 \exp(-E_\gamma/T)$. (b) Dipole and quadrupole soil components (full line) corrected for angular distributions and Doppler shifts; corresponding spectra from the ^{120}Sn(^{36}S, 4n) reaction are shown as dashed lines (c) Sum of soil and grass parts observed at 0° and 147°. (d) Ratio of the spectra in (c) (147°/0°) compared with model calculations discussed in the text (dashed line).

ponent, like the trees and grass, does not show any energy shift, i.e. is mainly emitted after the residual nucleus has stopped in the backing. In contrast, the upper edge of the E2 bump (figs. 1c and 1d) and the statistical tail above 2 MeV are both nearly fully shifted, providing that their decay times are much shorter than the stopping time and that the quadrupole soil precedes the dipole soil in the decay. Using the established time ordering, and also the feeding times of the yrast states [1,2], the average decay path (fig. 2a) can be reconstructed from the values of $\overline{\Delta E}$ and $\overline{\Delta I}$ listed in table 1. The ordering of the E2 soil and the statisticals is highly schematic and does not reflect the fact that they are actually interleaved, as discussed below. It is clear that the dipole and the quadrupole parts of the quasicontinuum display very different properties: the former is slow and nearly independent on the input spin I, whereas the latter is very fast, with a multiplicity increasing with I.

The E2 and statistical; lifetimes were determined by fitting the data with a simple model that takes into account the competition between in-band collective E2 transitions and out-of-band statistical E1 decay at high excitation energy and spin. Its basic ingredients are: (i) statistical E1 decay governed by the level densities [11] and the giant dipole resonance strength function based on the classical energy-weighted sum rule; and (ii) collective bands characterized by a transition quadrupole moment Q_t, an effective moment of inertia $\mathcal{I}_{\rm eff}$ and a cut-off energy U_0, which is required to account for our observation that the single particle grass and dipole soil components represent the last stages in the feeding of the yrast line. A value of $U_0 \sim 1.5$ MeV was determined from the internal excitation energy corresponding to the starting point of the dipole soil "vector" – see fig. 2a. γ cascades were generated in a Monte Carlo procedure based on this model, starting from an entry region centered around the *measured* average entry points given in table 1. The initial (gaussian) spreads in spin [$\sigma(I) = 5\hbar$] and excitation energy [$\sigma(E) = 2.5$ MeV] are taken in agreement with typical spin-distribution data [12]. Along the cascade, each level is allowed to decay either by an in-band collective E2 or an out-of-band statistical E1 transition. A spreading of the rotational strength is included, with the spreading width [13] $\Gamma_{\rm rot} = 200$ keV. Finally, the collective cascades are terminated when U drops

Table 1
Average properties of the γ-ray components feeding the 60 ns ($I=17^-$) isomer in ^{152}Dy.

	^{36}S+^{120}Sn			^{82}Se+^{76}Ge		
	$\overline{M_\gamma}$	$\overline{\Delta I_i}$ ($\hbar$)	$\overline{\Delta E_i}$ (MeV)	$\overline{M_\gamma}$	$\overline{\Delta I_i}$ ($\hbar$)	$\overline{\Delta E_i}$ (MeV)
trees	10.7	15.2	5.75	11.8	16.6	6.74
grass	1.5	2.3	1.35	1.9	3.4	2.23
dipole soil	1.4	1.4	0.85	1.3	1.3	0.77
quadrupole soil	4.4	8.8	5.22	7.2	14.4	9.20
statisticals	4.0	2.0	7.36	3.9	1.9	7.79
total	22.0	29.7	20.53	26.1	37.6	26.73
$\bar{I}_{in}$ [a], $\bar{E}_{in}$ [b]	46.7 $\hbar$, 25.6 MeV			54.6 $\hbar$, 31.8 MeV		

[a] $\bar{I}_{in}=I_{17^-}+\sum\overline{\Delta I_i}$. [b] $\bar{E}_{in}=E_{17^-}+\sum\overline{\Delta E_i}$.

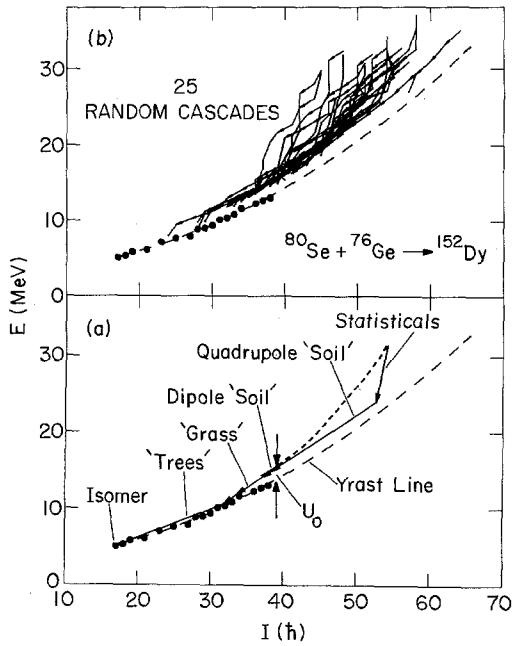

Fig. 2. (a) Schematic representation of the γ-decay path for the ^{67}Ge(^{80}Se, 4n)^{152}Dy reaction, using $\overline{\Delta I_i}$ and $\overline{\Delta E_i}$ values from table 1. Known yrast states (circles) and the extrapolated yrast line (long dashed) are shown. The collectivity is cut off at energies $U<U_0$, as discussed in the text. (b) Same as (a), but with a sample of simulated cascades, generated using $Q_t=7\,e$ b, $\mathcal{I}_{eff}=76\,\hbar^2$ MeV^{-1} and $a=A/7$. The resulting average deexcitation flow is indicated in (a) by the short-dashed line.

below U_0. A sample of simulated cascades is shown in fig. 2b and can be compared with the average measured decay path in fig. 2a. An important aspect of this model is that it can *simultaneously* reproduce the experimentally measured Doppler shifts, multiplicities, and spectral shapes for both E2 soil and statistical components with a unique set of parameters: $\mathcal{I}_{eff}$, Q_t and a. $\mathcal{I}_{eff}$ is determined by the average rotational transition energy, i.e. the centroid of the E2 bump, Q_t by the Doppler shift of the bump in the backed targets, its multiplicity and spectral shape, and a the level density parameter, mainly by the shape of the statistical tail, its Doppler shift and multiplicity. Fig. 1d compares the experimental and simulated ratios of the 147° and 0° E2 soil spectra for the ^{80}Se+^{76}Ge reaction. Fitting the model to the data for both reactions yields $a=A/(7\pm1)$ MeV^{-1}, $\mathcal{I}_{eff}=76\,\hbar^2$ MeV^{-1} (with an assumed gaussian spread of $\sigma=5$) and $Q_t=7.0^{+2.5}_{-1.5}\,e$ b, the last value in agreement with the findings by Hübel et al. of $5.4\pm3.0\,e$ b in ^{152,153}Er [6].

It has, for the first time, been possible to fully reconstruct and quantify the detailed gamma deexcitation process of a nucleus. After neutron evaporation, the residual nucleus decays by γ-ray emission through a cascade of interleaved statistical E1 and fast collective E2 transitions. The former mainly cool the nucleus towards the yrast line and predominate at higher temperature, and the latter remove angular momentum with little cooling. If an axially symmetric prolate rotor is assumed (although in principle non-axial shapes are allowed), the measured Q_t values imply a deformation of $\beta=0.32$. Thus, the bulk of these collective bands are not associated with superdeformed shapes ($\beta\sim0.6$), but have defor-

mation similar to those observed in neighboring prolate nuclei. The collective cascades extend over a fairly large range in spin (at least from $I=35$ to $55\hbar$), and our model calculations suggest that they tend to be concentrated in a region 1.5–3.5 MeV above the yrast line (see fig. 2b); they are observed to be absent below $U=1$–1.5 MeV, a feature correctly predicted by theory [7]. From that point, the decay continues predominantly through slow transitions between single-particle states, which generate the dipole soil. This is inferred from its long decay times and its invariance with the input spin, a behaviour in striking contrast to that of the quadrupole soil. With decreasing level density, the continuum gives way to many sharp lines, represented by the grass component, and finally the yrast transitions. The last, non-collective part of the decay into the yrast line is not calculated here because it requires knowledge of all levels and transition probabilities. However, model calculations by Åberg et al. [14], who treat only transitions between single-particle states, yield spectra in reasonable agreement with the sum of our grass and dipole soil components.

Thus, in nuclei with aligned-particle states in the yrast region, the deexcitation flow is dominated by collective cascades similar to the decay in so-called "good" rotors for $U>1.5$ MeV. There may be a generic relationship between these bands and those in the more deformed neighboring nuclei, but this possibility needs further examination. The proposed deexcitation picture can be generalized to nuclei with prolate yrast states by removing the collectivity cutoff U_0; this results in a continuation of the collective flow above the yrast line and a feeding into it at significantly lower spins—in accord with observation [15].

References

[1] B. Haas et al., Nucl. Phys. A 362 (1981) 284.
[2] F. Azgui et al., Nucl. Phys. A 439 (1985) 573.
[3] B.M. Nyakó et al., Phys. Rev. Lett. 56 (1986) 2680.
[4] P.J. Twin et al., Phys. Rev. Lett. 57 (1986) 811.
[5] P. Chowdhury et al., Phys. Rev., Lett. 47 (1981) 1788; D. Ward et al., Nucl. Phys. A 397 (1983) 161.
[6] H. Hübel et al., Phys. Rev. Lett. 41 (1978) 791; Z. Phys. A 304 (1982) 225.
[7] H.J. Riezebos et al., Phys. Lett. B 183 (1987) 277.
[8] D.C. Radford et al., Phys. Rev. Lett. 55 (1985) 1727.
[9] R. Holzmann et al., to be published.
[10] D.C. Radford et al., to be published.
[11] A. Bohr and B.R. Mottelson, Nuclear structure, Vol. 1 (Benjamin, New York, 1979) p. 155.
[12] R.D. Fischer et al., Phys. Lett. B 171 (1986) 33.
[13] J. Bacelar et al., Phys. Rev. Lett. 55 (1985) 1858; F.S. Stephens et al., Phys. Rev. Lett. 57 (1986) 2912.
[14] S. Åberg et al., Nucl. Phys. A 443 (1985) 91.
[15] J. Borggreen et al., Nucl. Phys. A 443 (1985) 120.